Available online at www.sciencedirect.com

SCIENCE DIRECT

Experimental Cell Research 298 (2004) 549–559

Experimental Cell Research

www.elsevier.com/locate/yexcr

Contribution of $p16^{INK4a}$ to replicative senescence of human fibroblasts

Sharon Brookes,[a,1] Janice Rowe,[a,1] Ana Gutierrez del Arroyo,[a] Jane Bond,[b] and Gordon Peters[a,*]

[a] *Cancer Research UK, London Research Institute, Lincoln's Inn Fields Laboratories, London WC2A 3PX, UK*
[b] *Department of Pathology, University of Wales College of Medicine, Cardiff CF14 4XN, UK*

Received 10 February 2004, revised version received 23 April 2004
Available online 25 May 2004

Abstract

In standard conditions of tissue culture, human fibroblasts undergo a limited number of population doublings before entering a state of irreversible growth arrest termed replicative senescence or M1. The arrest is triggered by a combination of telomere dysfunction and the stresses inflicted by culture conditions and is implemented, at least in part, by the cyclin-dependent kinase inhibitors $p21^{CIP1}$ and $p16^{INK4a}$. To investigate the role of $p16^{INK4a}$, we have studied fibroblasts from members of melanoma prone kindreds with mutations in one or both copies of the *CDKN2A* locus. The mutations affect the function of $p16^{INK4a}$ but not of the alternative product, $p14^{ARF}$. The $p16^{INK4a}$-defective fibroblasts have an above average life span, compared to the heterozygous and normal age-matched controls, but they arrest with characteristics typical of senescence. Using agents that are known to bypass M1, such as DNA tumor virus oncoproteins or the Bmi1 transcriptional repressor, we provide evidence that $p16^{INK4a}$ defective cells arrest at a stage that is operationally between M1 and M2 (crisis). As well as indicating that $p16^{INK4a}$ contributes to but is not essential for replicative senescence of human fibroblasts, our data reveal considerable heterogeneity in the levels and accumulation of $p16^{INK4a}$ in different strains.

Keywords: INK4a; ARF; Senescence; Crisis; Human fibroblasts; Bmi1; Telomeres

Introduction

Replicative senescence was first described in cultures of primary human diploid fibroblasts, and because of its experimental tractability this cell system remains a popular model in which to study the underlying mechanisms [1]. After what appears to be a predetermined number of population doublings, fibroblasts enter a state of growth arrest, called M1 [2], characterized by a flattened morphology, negligible BrdU labeling and increased senescence-associated β-galactosidase (SA-βgal) activity [3,4]. A critical determinant of M1 is the erosion of the telomeres that occurs with each division in cells lacking telomerase activity [5–7]. Ectopic expression of hTERT, the catalytic component of telomerase, can preempt the effects of telomere loss and under appropriate conditions enables human fibroblasts to proliferate indefinitely [8,9].

However, the ability of hTERT to immortalize human cells is not universal and it is now appreciated that there are telomere-independent mechanisms that limit proliferative life span [10]. For example, some human epithelial cell types undergo a senescence-like arrest after a relatively small number of population doublings and before telomere erosion has reached critical proportions [11–16]. As the timing of this arrest can vary, depending on the culture conditions and the cell type [14], there is a cogent argument that the arrest occurs as a consequence of stresses imposed by tissue culture [10,17]. Deliberate stressing of cells, for example, with high oxygen tension, DNA damaging agents or with activated oncogenes, can elicit a similar senescence-like arrest [18–23], for which we have suggested the term stasis [24].

In addition to the phenotypic similarities between stasis and senescence, there are common elements in the underlying mechanisms. The available evidence indicates pivotal roles for the retinoblastoma (pRb) and p53 tumor suppressor pathways [25,26], with the arrest being primarily imple-

* Corresponding author. Lincoln's Inn Fields Laboratories, London Research Institute, 44 Lincoln's Inn Fields, London WC2A 3PX, UK. Fax: +44-207-269-3094.
E-mail address: gordon.peters@cancer.org.uk (G. Peters).
[1] The first two authors made equal contributions to this study.

0014-4827/$ - see front matter © 2004 Elsevier Inc. All rights reserved.
doi:10.1016/j.yexcr.2004.04.035

mented by the cyclin-dependent kinase inhibitors $p16^{INK4a}$ and $p21^{CIP1}$ [27–30]. Agents that inactivate p53 and pRb, such as SV40 large tumor antigen (T-Ag) or the human papillomavirus (HPV) E6 and E7 proteins, enable fibroblasts to bypass M1 [25]. However, the continued erosion of telomeres during this period of extended life span eventually leads to chromosome fusion and breakage and the cultures reach a state called M2 or crisis where cell division is still occurring, as judged by BrdU incorporation, but is offset by extensive cell death [2,3]. Expression of hTERT can rescue cells from crisis [31,32].

There is considerable interest in the role of $p16^{INK4a}$ in senescence and how this relates to its properties as a tumor suppressor. Whereas $p21^{CIP1}$ levels peak just before M1, consistent with the initiation of the senescence arrest, $p16^{INK4a}$ shows more dramatic accumulation in cells that have reached M1 and changed their phenotypic characteristics [27,28,30]. These changes have been likened to differentiation and it now appears that the up-regulation of $p16^{INK4a}$ may be responsible for making the arrest irreversible [30,33]. Significantly, most established human cell lines lack functional $p16^{INK4a}$, because of mutation, deletion or epigenetic silencing of the gene, underscoring its importance in limiting cell proliferation [34]. Similar alterations occur in primary cancers, albeit less frequently. Such observations suggest that deliberate ablation of $p16^{INK4a}$ could facilitate the bypass of senescence and there have been many studies that have approached this issue, for example, by overexpression of Cdk4, the principal target of $p16^{INK4a}$ [35,36], or the Bmi1 transcriptional repressor [37,38] and more recently with antisense constructs [39] or short interfering RNA against $p16^{INK4a}$ [33,40–43].

As an alternative strategy, we have been investigating fibroblasts derived from rare individuals carrying germline mutations in both alleles of the *INK4a/ARF* locus [44,45]. These have the advantage that $p16^{INK4a}$ is constitutively inactive rather than experimentally suppressed and that ARF, the alternative product encoded by this locus, remains functional. Our findings suggest that $p16^{INK4a}$ contributes to but is not essential for the termination of fibroblast life span. Importantly, the $p16^{INK4a}$-deficient cells arrest at a stage that is intermediate between M1 and M2. By comparing $p16^{INK4a}$-deficient cells with other primary fibroblast strains, including those with heterozygous mutations in *INK4a/ARF*, we show that there is considerable variability in the basal levels and kinetics of accumulation of $p16^{INK4a}$ in different strains.

Materials and methods

Cells and culture conditions

F003 and Leiden cells were obtained from Nico Smit, Wilma Bergman and Nelleke Gruis, Leiden University Medical Centre, The Netherlands. The ESC cells were isolated from an endometrial biopsy provided by Dr. Jan Brosens, Hammersmith Hospital, London, UK. IDF cells were provided by Jean-Laurent Casanova, Necker-Enfants Malades Medical School, Paris, France. Q34, ADF and FDF cells were supplied by Veronique Bataille and Anthony Quinn, Royal London Hospital, London, UK. MI6 cells were isolated and generously donated by Dr. Marie-Françoise Avril and Dr. Laurent Ferradini, Institut Pasteur, Paris, France. The TIG3 strain of embryonic lung fibroblasts and the Hs68 strain of neonatal foreskin fibroblasts (ATCC: CRL 1635) have been described previously [44].

Cell stocks were maintained at 37°C and 5% CO_2 in Dulbecco modified Eagle's medium (DMEM) supplemented with 10% fetal calf serum (FCS). The fibroblast cultures were routinely passaged at a 1:4 split ratio as soon as they reached confluence and were therefore assumed to have undergone 2 PDs at each passage.

Retroviral infection and selection

Each fibroblast strain was rendered sensitive to mouse ecotropic retroviruses by infecting with amphotropic retroviruses encoding the mouse basic amino acid transporter and thereafter maintained in medium containing 150 μg/ml G418 as previously described [29]. Ecotropic retroviral stocks were prepared by transient transfection of BOSC-23 cells. For retroviral infections, fibroblasts expressing the ecotropic receptor were plated at 25–50% confluence and incubated overnight. The culture medium was replaced with 5 ml of filtered viral supernatant together with 3 ml of fresh medium and the equivalent of 4 μg/ml polybrene. After 24 h, the medium was replaced and selection in medium containing either 1.25 μg/ml puromycin (Calbiochem) or 50–100 μg/ml hygromycin (Sigma) was initiated on day 2 postinfection.

The pBABE retroviral vectors encoding SV40 large T-antigen and HPV-16 E6 have been described previously. A similar retroviral vector encoding human Bmi1 was kindly provided by Maarten van Lohuizen.

Protein analyses

Cells were lysed in 62.5 mM Tris–HCl (pH 6.8) containing 2% w/v SDS and the protein concentration using the BCA assay (Pierce). Mercaptoethanol and bromophenol blue were added to make the final composition equivalent to Laemmli sample buffer. Samples were fractionated by SDS-polyacrylamide gel electrophoresis (SDS-PAGE) and blotted onto Immobilon-P membrane (Millipore) and processed as previously described [46]. Depending on the experiment, sheep anti-mouse HRP (1:1000 dilution) and donkey anti-rabbit HRP (1:2000 dilution) were used as secondary antibodies (Amersham). Antibody binding was visualized using Amersham ECL reagents. The monoclonal antibody DO-1 (sc-126) against p53 and rabbit polyclonal

Table 1
Characteristics of different human fibroblast strains

Cell strain	Source	CDKN2A status	Life span PDs	
TIG3	fetal lung	normal	72–73	≥3 C
FDF	fetal skin	normal	77–80	≥3 C
Hs68	neonatal skin	normal	65–69	≥3
IDF	infant skin	normal	55–63	≥3
ADF	adult skin	normal	12–14	1
904	adult skin	normal	28–34	≥3
ESC	adult endometrium	normal	40–43	≥3 C
FEO2	adult skin	normal	46–58	≥3
MI6	adult skin	heterozygous mutation	50–52	2
F003	adult skin	heterozygous mutation	42–45	2
Leiden	adult skin	homozygous mutation	60–63	≥3
Q34	adult skin	biallelic mutations	80–88	≥3

Numbers in the right column indicate the number of independent life span measurements conducted. C = strains that show the "classical" pattern of $p16^{INK4a}$ accumulation at M1 (see Fig. 5).

antibodies against Cdk4 (sc-601) and $p21^{CIP1}$ (sc-397) were obtained from Santa Cruz. Rabbit polyclonal antisera against MEK1/2 (#9122) and phospho MEK (#9121S) were from Cell Signalling and monoclonal antibodies against $p16^{INK4a}$ (DCS50 and JC8) have been described previously [44].

Immunohistochemical staining and fluorescence

For fluorescence detection, cells were grown on glass coverslips. Apoptosis was assessed using the ApoAlert™ system (Clontech) to detect surface binding of FITC-conjugated Annexin V, as described by the supplier. BrdU incorporation was measured using an immunohistochemical assay system (Boehringer Mannheim 1299 964) as previously described [44]. Immunohistochemical detection of $p16^{INK4a}$ and Ki67 was achieved using the Doublestain system (DAKO) following the protocols recommended by the manufacturer. For dual detection, $p16^{INK4a}$ was visualized with the JC8 mouse monoclonal antibody followed by alkaline phosphatase-based secondary reagents, whereas Ki67 was detected with a rabbit polyclonal antibody followed by a horseradish peroxidase secondary system.

Results

INK4a-deficient human fibroblasts undergo M1-like senescence

We have previously described strains of primary dermal fibroblasts derived from melanoma prone kindreds with germline *CDKN2A* mutations. The first example, designated Leiden (Table 1), was from an individual who is homozygous for a 19-bp deletion in exon 2 [47]. The resultant frameshift creates two distinctive fusion proteins, neither of which can function as a Cdk inhibitor [44]. In contrast, one of the fusion proteins retains the amino terminal domain of ARF that is both necessary and sufficient for its known functions. A second fibroblast strain (designated F003) was obtained from a first-degree relative of the Leiden patient and biochemical analyses confirm the presence of both wild-type and mutant proteins [44]. A third strain (designated Q34) was isolated from an individual with different missense mutations in each *CDKN2A* allele [45]. Both mutations impair the function of $p16^{INK4a}$, albeit to different extents, but only one changes the primary sequence of ARF (Table 1). Functional evaluation indicated that it has no discernible effect on the properties of ARF [45]. A fourth strain (MI6) was isolated from a heterozygous individual with a germline insertion in exon 1α. The mutation, 19insTA, causes severe impairment of $p16^{INK4a}$ function as judged by Cdk4-binding and cell cycle arrest assays (data not shown) but by definition has no effect on $p14^{ARF}$.

As controls for these $p16^{INK4a}$-deficient strains, all of which were dermal fibroblasts from adult donors, we studied representative strains of dermal fibroblasts from adult (ADF, 904 and FEO2), infant (IDF), neonatal (Hs68) and fetal (FDF) sources that have no known *CDKN2A* defects (Table 1). Finally, we used the TIG3 strain as an example of the fetal lung fibroblasts on which classical models of senescence have been based, and a strain of adult endometrial stromal fibroblasts (ESC) as an additional non-dermal control. As these primary fibroblasts originated from different laboratories, there is some uncertainty about the number of population doublings that occurred before the first passage. However, their subsequent passage history is well documented. Upon transfer to our laboratory, they were propagated according to the same standard protocol until the cultures failed to double in 4–5 weeks. Typical growth curves for eight dermal fibroblast strains are shown in Fig. 1. Although some of the strains (e.g. FDF) conformed to the classical model of logarithmic proliferation culminating in an almost synchronous arrest, others showed a more gradual decline in proliferation rate. Importantly, all of the strains, including the $p16^{INK4a}$-deficient Leiden and Q34 fibroblasts, entered an M1-like state, as judged by negligible BrdU incorporation and positive staining for SA-βgal (data not shown).

Do $p16^{INK4a}$-deficient fibroblasts have an extended life span?

Although much of the literature on senescence holds that the replicative life span of cells in tissue culture is inversely related to the age of the donor, a recent reevaluation that included repeated biopsies from the same individuals found no significant correlation with donor age [48]. Nevertheless, fibroblasts from embryonic sources generally have higher initial growth rates and longer life

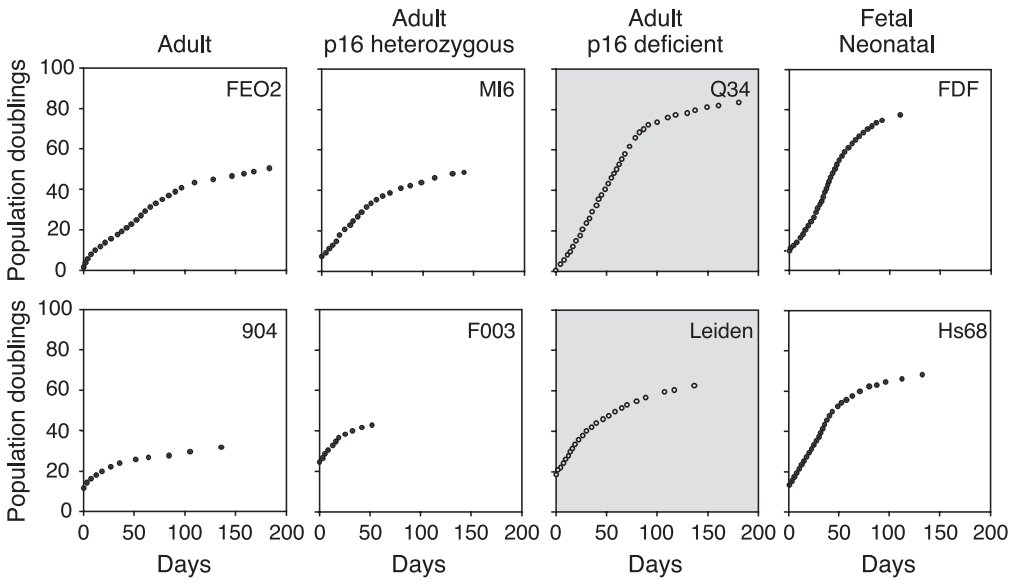

Fig. 1. Limited life spans of different strains of dermal fibroblasts. Each panel shows the cumulative populations doublings (PDs) achieved by the indicated strain of human fibroblast as a function of time. The two $p16^{INK4a}$-deficient strains are identified by the grey background. Note that depending on the source of the cells, the zero time points reflect different numbers of PDs. The results are representative of several independent growth curves as summarized in Table 1.

spans than cells from adult donors [48–51]. Thus, fibroblasts from fetal sources typically proliferate for between 50 and 90 PDs, with a median of around 70 PDs, whereas fibroblasts from adult sources have recorded life spans of between 10 and 70 PDs, with a median of around 35–40 PDs (Fig. 2). In agreement with these distributions, the fetal cells included in our study (TIG3 and FDF) achieved 73 and 80 PDs, respectively, whereas the majority of the adult cells reached senescence after 30–50 PDs, including the two strains (F003 and MI6) that are heterozygous for $p16^{INK4a}$ mutations. The only exceptions were the two $p16^{INK4a}$-deficient stains, Leiden and Q34, which reached senescence after 60 and 88 PDs, respectively. Although it could be argued that the Leiden cells are at the upper limit of the norm for adult fibroblasts, the life span of the Q34 cells is well above this limit.

These results suggested but did not prove that M1 is delayed in the $p16^{INK4a}$-deficient cells. To investigate this possibility, we asked whether the HPV E6 protein or SV40 T-Ag would cause life span extension in Leiden and Q34 cells comparable to that seen in normal fibroblasts. The cells were first infected with an amphotropic retrovirus encoding the mouse basic amino acid transporter, which rendered them sensitive to infection by ecotropic retroviruses [29]. Empty vector controls were included for each infection. As well as counting the

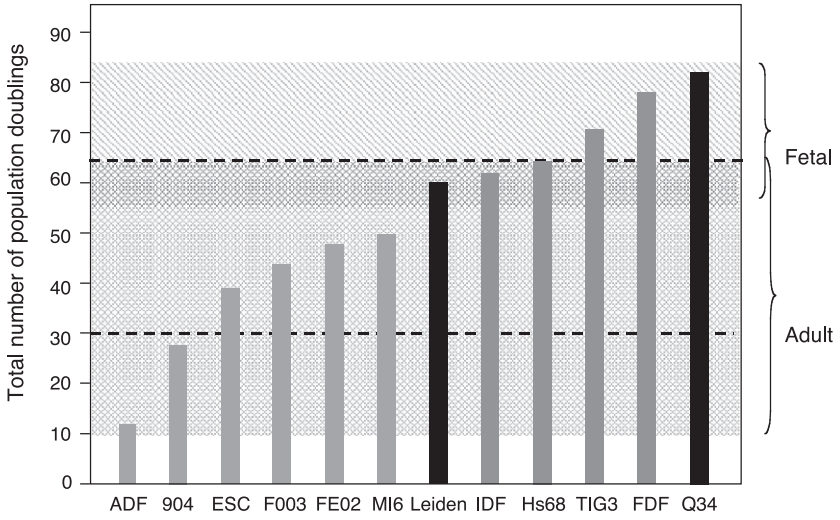

Fig. 2. Comparison of the maximum life spans of different human fibroblast strains. The histogram shows the average number of PDs achieved by each strain of fibroblast (see Table 1) plotted against background shading that represents the typical life span ranges for fibroblasts from adult (crosses) and fetal (diagonal lines) sources. The dashed lines indicate the median life span for adult (lower) and fetal (upper) fibroblasts as deduced from published studies [48–51].

maximum number of PDs achieved by each cell pool, we also determined whether the cultures eventually acquired an M1 or M2 phenotype by monitoring for BrdU incorporation and annexin staining; M2 cultures show significant levels of DNA synthesis and apoptosis. In line with expectations, introduction of SV40 T-Ag, which targets both pRb and p53, extended the life span of each fibroblast strain by between 20 and 30 PDs (Fig. 3), and the cultures invariably underwent M2 (crisis). There were no obvious differences between the $p16^{INK4a}$-deficient and wild-type cells in the degree of life span extension, which can be quite variable. Cells expressing HPV E6, which targets p53, also had extended life spans (typically 15 to 20 PDs) but there was a clear distinction in the eventual arrest phenotype. Whereas normal fibroblasts, whether from adult or fetal sources, acquired an M1-like phenotype, E6 enabled the two $p16^{INK4a}$-deficient strains to proceed directly to M2 (Fig. 3). These results would be consistent with the idea that the $p16^{INK4a}$-deficient strains arrest at an intermediate stage between M1 and M2, which we operationally refer to as M1.5. Although phenotypically similar to the M^{Int} state caused by disabling the p53/p21 axis with E6 [52], the underlying mechanisms must be different.

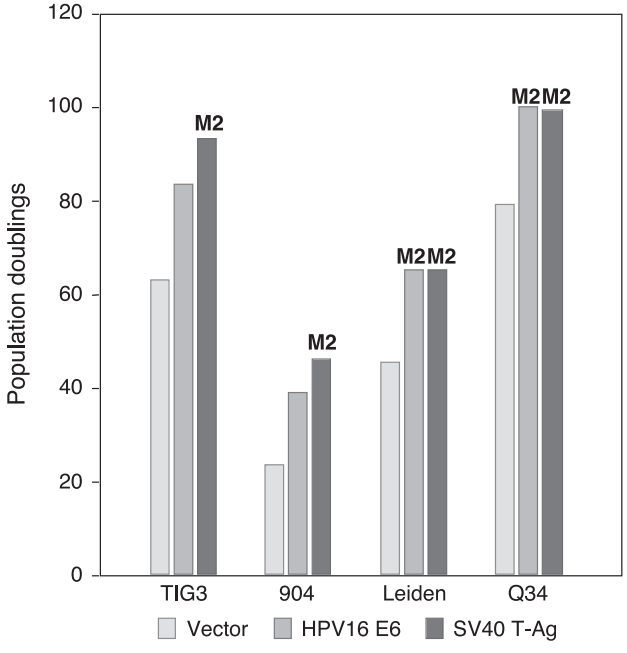

Fig. 3. Life span extension of normal and $p16^{INK4a}$-deficient fibroblasts. The histograms compare the maximum PDs achieved by the indicated strains of fibroblast infected with retroviruses encoding SV40 T-antigen, HPV E6 or empty vector control. M2 identifies cultures that underwent crisis, as determined by BrdU incorporation and cell death [3]. Note that the control cells have reduced life spans compared to the values indicated in Fig. 2. In our hands, introduction of the basic amino transporter (ecotropic receptor) into human fibroblasts equates with a loss of approximately 5 PDs relative to uninfected parental cells. The data shown represent the average of two independent experiments.

Bmi1 does not extend the life span of $p16^{INK4a}$-deficient fibroblasts

To gain further support for this idea, we also investigated the effect of the polycomb protein Bmi1, which can suppress *INK4a* expression resulting in a partially extended life span [37,38]. For example, the TIG3 and 904 strains infected with a Bmi1-encoding retrovirus proliferated for an additional 10–12 PDs relative to the empty vector controls, culminating in an M1-like phenotype (Fig. 4A and data not shown). Although the $p16^{INK4a}$ levels were substantially reduced in the Bmi1-transduced pools, there was still a noticeable accumulation of the protein at senescence (Fig. 4C). In TIG3 cells, the life span extension afforded by Bmi1 was less than that observed in cells expressing E6. However, as recently shown [38], the effects were additive and TIG3 cells expressing both Bmi1 and E6 achieved an additional 30 PDs (Fig. 4A). In contrast, in Leiden and Q34 cells, Bmi1 provided negligible life span extension and had no additional effect in the presence of E6 (Fig. 4B and data not shown). These findings agree with the idea that Bmi1 counteracts senescence primarily through its ability to suppress $p16^{INK4a}$ [37,38].

Contrasting patterns of senescence in different fibroblast strains

As well as monitoring population doublings in our panel of human fibroblasts, we also compared the levels and kinetics of $p16^{INK4a}$ and $p21^{CIP1}$ accumulation. Whereas many strains (TIG3, FDF and ESC) conformed to the "classical" pattern observed in published studies on embryo-derived fibroblasts, with a peak of $p21^{CIP1}$ expression preceding the pronounced accumulation of $p16^{INK4a}$ at M1 (see Fig. 5A), others showed a quite different pattern. Indeed, most of the strains we analyzed showed substantially increased $p21^{CIP1}$ and $p16^{INK4a}$ levels relatively early in their passage history, and the levels remained constant or declined during the remainder of the life span (Figs. 5B and C). These distinctions did not simply reflect differences in projected life span as the ESC cells chosen to exemplify the classical pattern in Fig. 5A reached senescence after only 43 PDs compared to 63 and 88 PDs for the IDF cells and Q34 cells; nor did they relate to variations in the basal levels of $p16^{INK4a}$ expressed by different strains. For comparative purposes, we analyzed equivalent amounts of total cellular protein prepared from cultures at approximately 50% of their projected life spans (Fig. 5D). Despite considerable variability, as noted in previous studies [33], there was no obvious trend that could account for the kinetics of $p16^{INK4a}$ accumulation.

We suspected that a more likely explanation would be heterogeneity in the cell cultures such that individual cells could undergo senescence at different times throughout the passage history of the culture. This could also explain the shape of the life span curves that monitor the proliferation of

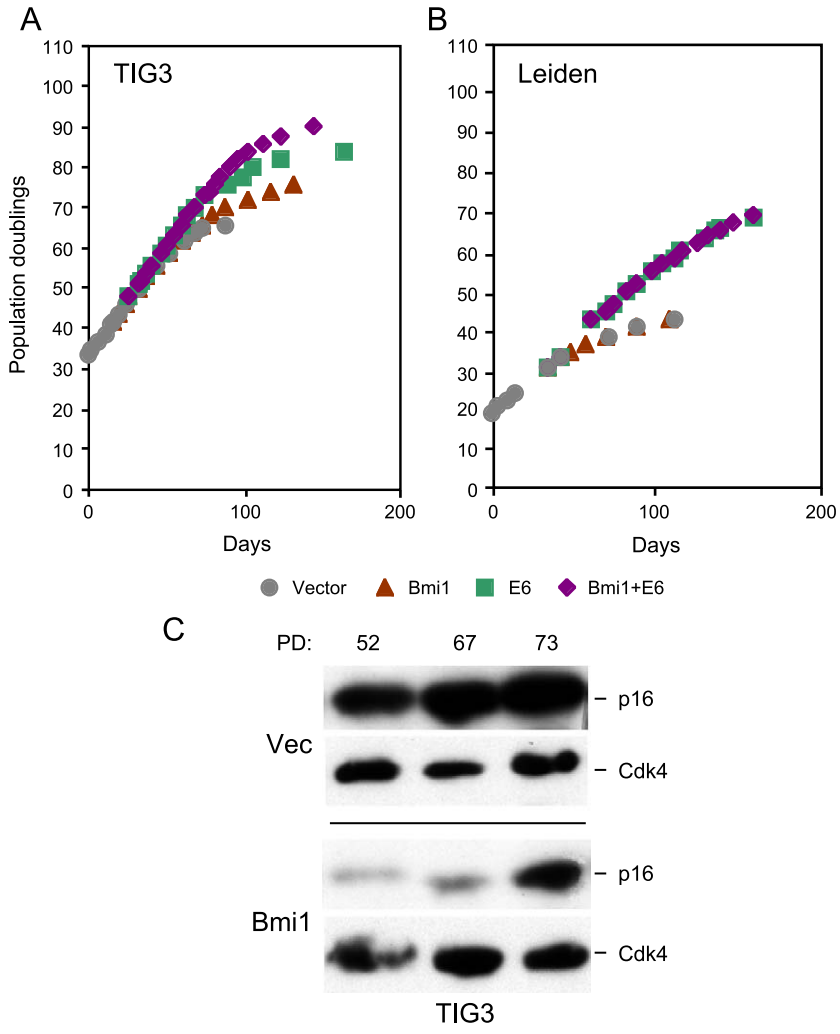

Fig. 4. Bmi1 does not extend the life span of p16^{INK4a}-deficient fibroblasts. TIG3 cells (A) and Leiden cells (B) were infected with retroviruses encoding Bmi1, HPV E6 or both, as indicated, along with empty vector controls. After drug selection, the cumulative PDs were monitored over time until the cultures failed to double in 4 weeks. Panel C shows the levels of p16^{INK4a} at the indicated PDs in TIG3 cells transduced with empty vector compared to those infected with the Bmi1 retrovirus. Cdk4 serves as the loading control for the immunoblot. The results are representative of at least two independent experiments.

the longest-lived cells. To investigate this possibility, we used immunohistochemical staining to assess the level of p16^{INK4a} in individual cells at different population doublings. The examples shown in Fig. 6 were selected to allow comparison between different strains at the approximate equivalent of 50%, 75% and 100% of their maximal life spans. In general, strong positive staining for p16^{INK4a} (red) was restricted to cells that had the enlarged, flattened appearance typical of senescence. These cells were negative for the proliferation marker Ki67 (brown) and in other fields corresponded to cells that expressed SA-βGal activity (not shown).

In "classical" fibroblast strains, such as TIG3 and FDF, there were very few p16^{INK4a}-positive cells at early and mid passage, but the proportion of positive cells increased at later passages and the staining became very pronounced at M1 (Figs. 6 and 7). There were obvious parallels between the increasing percentages of p16^{INK4a}-positive cells and the total levels of p16^{INK4a} protein detected by immunoblotting. In contrast, other fibroblast strains, such as 904 and IDF, showed a significant proportion of p16^{INK4a}-positive cells at only 50% of their passage history and the intensity of staining was generally lower than in senescent TIG3 cells (Fig. 6). In line with the immunoblotting data, the proportion of p16^{INK4a}-positive cells increased at early passages and then remained relatively constant throughout the remainder of the life span (Fig. 7).

Discussion

The concept of replicative senescence has prompted long and often contentious debates about the relationship between cell and/or culture life span and the age and/or longevity of the donor, amid continuing concerns that tissue culture is very artificial in terms of oxygen tension,

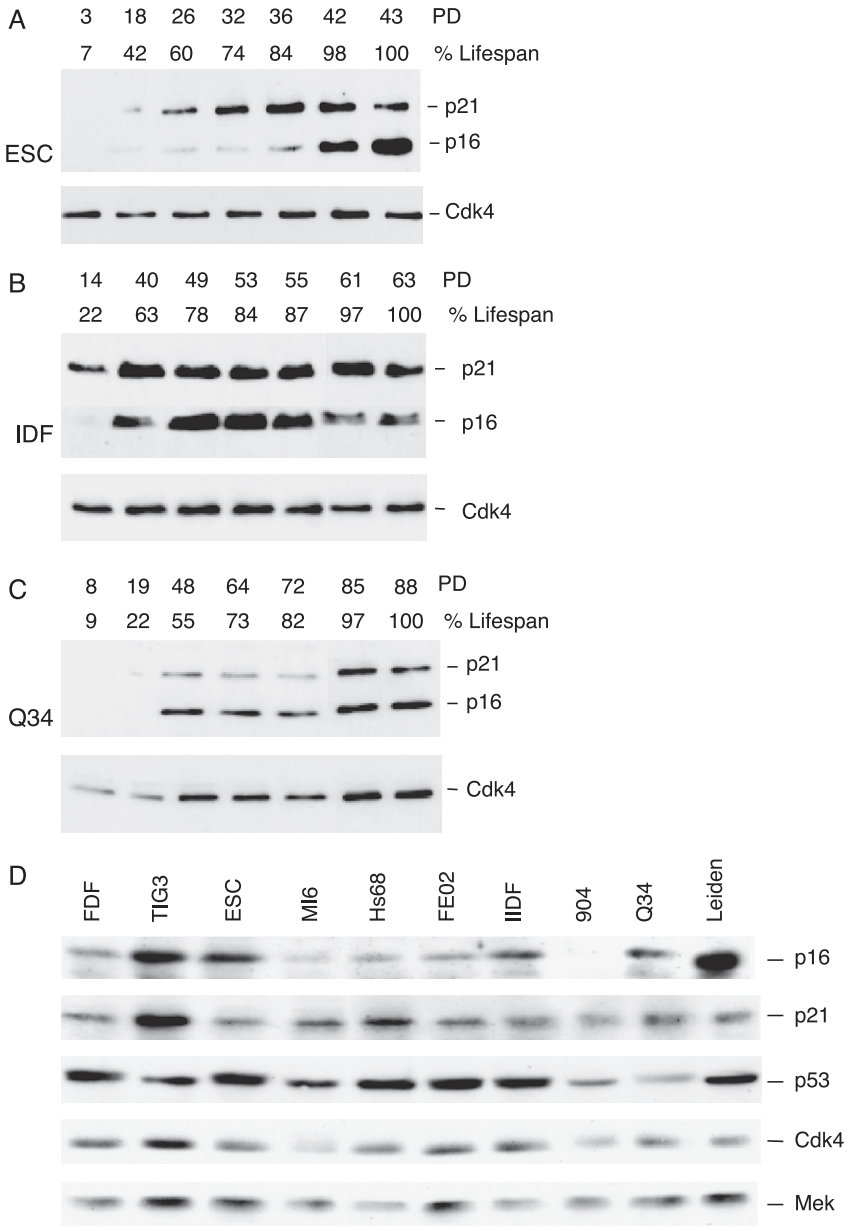

Fig. 5. Kinetics of $p16^{INK4a}$ and $p21^{CIP1}$ accumulation in different strains of human fibroblasts. Total cell lysates were prepared at different population doublings throughout the life span of each cell strain and equivalent samples (20 μg protein) were analyzed by immunoblotting for $p16^{INK4a}$, $p21^{CIP1}$ and Cdk4 as indicated. Numbers above the lanes indicate the population doubling of each sample and how this relates to the projected life span. (A) ESC cells. (B) IDF cells. (C) Q34 cells. (D) Comparison of the total levels of $p16^{INK4a}$ and other relevant proteins in different fibroblast strains at approximately 50% of their projected life spans; 20-μg samples of protein in each case.

substratum and the provision of growth and survival factors. Despite these concerns, experimental dissection of senescence has been highly informative about the importance of telomere status and the pRb, p53 and $p16^{INK4a}$ tumor suppressors in limiting the proliferative potential of somatic cells. Most attempts to study the phenomenon in human cells have involved deliberate ablation of the critical components, either by introduction of DNA tumor virus proteins, dominant negative mutants, antisense strategies and recently the use of siRNA [2,26,33,35,39–43,53]. Exceptionally, specific strains of human fibroblasts have been developed in which key genes have been targeted by homologous recombination, and spontaneously arising cell clones have been observed in which the $p16^{INK4a}$ gene has been silenced [42,54–56]. The approach we have taken is to analyze fibroblasts from individuals with inactivating mutations in both alleles of $p16^{INK4a}$, an important advantage being that these cells have never experienced functional $p16^{INK4a}$ at any stage in their life span.

A key finding is that the $p16^{INK4a}$-deficient fibroblasts have a finite life span that terminates at an intermediate

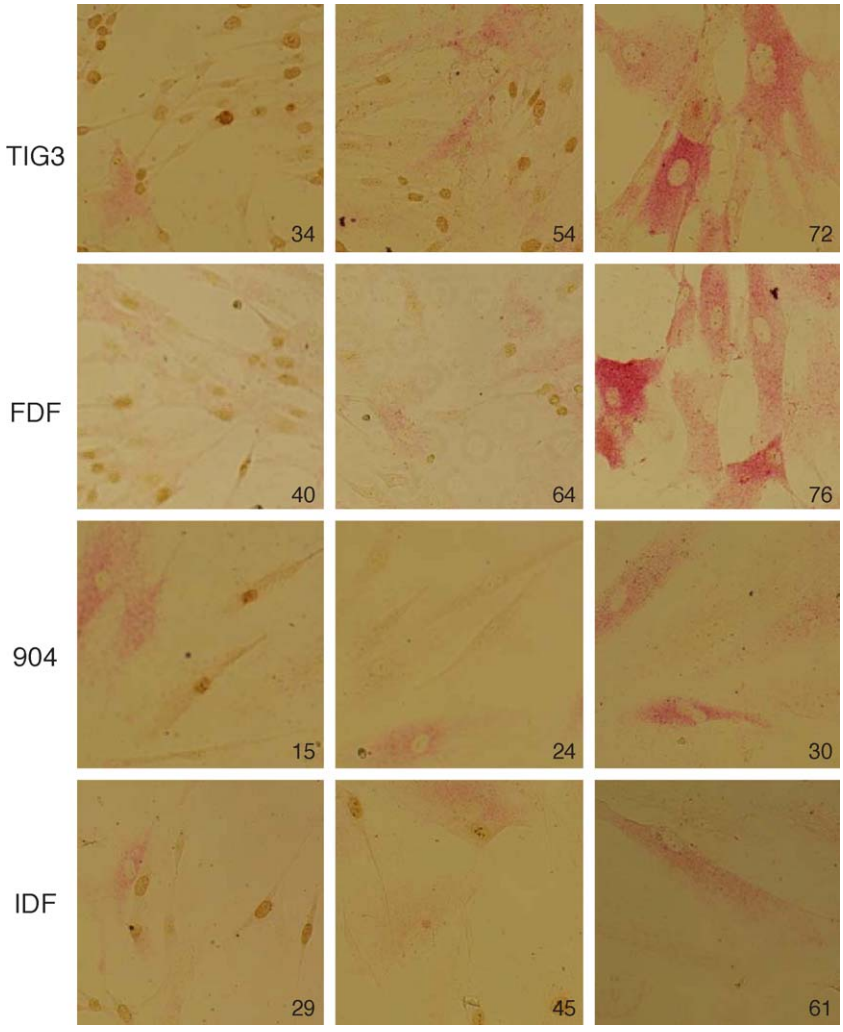

Fig. 6. Heterogeneity of $p16^{INK4a}$ expression throughout the life span of human fibroblasts. Immunohistochemical staining for $p16^{INK4a}$ using the JC8 antibody and alkaline phosphatase secondary detection system (red) and for Ki67 using HRP-based detection (brown). The numbers in each panel refer to the population doubling of the cell.

stage between M1 and M2. Predictably, agents that target the p53/p21 axis enable these cells to proceed to M2, whereas agents that target pRb/p16 have no effect on their replicative life span. These observations are consistent with an emerging model in which fibroblast life span is largely determined by the combined effects of telomere erosion and culture stress [10]. Although mechanistic details remain sparse, it seems reasonable to assume that telomere dysfunction eventually registers as DNA damage, triggering among other things the activation of p53 and $p21^{CIP1}$-mediated growth arrest. The consequences of oxidative stress also appear to be routed via p53/p21 [38]. However, the impact of $p21^{CIP1}$ on cell cycle progression is complicated by its ability to associate with a variety of different cyclin–Cdk complexes in both stimulatory and inhibitory roles [57]. Thus, the efficiency with which $p21^{CIP1}$ can enforce a senescence-like arrest will be heavily influenced by the availability of $p16^{INK4a}$ and potentially of other INK4 proteins that can sequester Cdk4 and Cdk6. When $p16^{INK4a}$ expression is reduced [37,38,42] or its function is compromised [33,35,42], the telomere-induced arrest is delayed.

One of the unexpected findings from our survey was that the simple model of temporally ordered $p21^{CIP1}$ and $p16^{INK4a}$ accumulation at senescence is not universally applicable. Thus, in the majority (approximately 75%) of the fibroblast strains we analyzed, the immunoblotting data would not support the conclusion that $p16^{INK4a}$ accumulates at the end of the proliferative life span of the culture. However, the correlation did appear to hold true at the level of the individual cell. Maximum staining for $p16^{INK4a}$ occurred in cells that looked visibly senescent whereas cells that were positive for the Ki67 proliferation marker showed minimal staining for $p16^{INK4a}$. In trying to interpret these findings, we considered two contrasting models. The simplistic assumption would be that the pattern of $p16^{INK4a}$ accumulation observed in the mass culture parallels the changes occurring in the individual cell. Using the ‘‘classi-

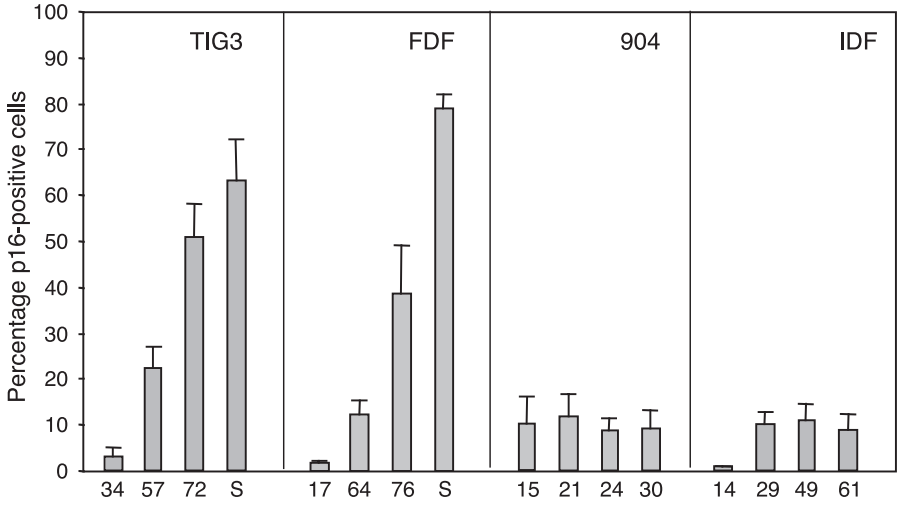

Fig. 7. Quantitation of immunostaining as a function of population doubling. The percentage of cells staining positive for $p16^{INK4a}$ at each time point was calculated by observing three random fields. The histograms show the average and standard deviation at the indicated PD.

cal" strains of fibroblast as a paradigm, this requires small gradual increments at early passages rising almost exponentially as the cell approaches M1. At present, we cannot provide a simple molecular explanation of how this could be achieved, although an indirect consequence of a telomere position effect remains a possibility [58]. The alternative model is that $p16^{INK4a}$ regulation operates essentially as a binary switch: the gene is either *OFF* or *ON*. In this scenario, techniques that measure average $p16^{INK4a}$ levels throughout a mass culture, such as immunoblotting, will monitor the proportion of the cells in which expression is *ON*. In practice, the *ON*/*OFF* distinction may not be absolute but could equate to high and low expression, as observed for example by immunohistochemical staining. Support for this concept comes from the correlation between the changing percentages of $p16^{INK4a}$-positive cells in Fig. 7 and the average levels detected by immunoblotting in Fig. 5.

If the latter model holds true, then the distinction between classical and nonclassical patterns of $p16^{INK4a}$ accumulation can be explained on the basis of heterogeneity within the cell pools. The more homogeneous populations will switch on $p16^{INK4a}$ expression at about the same point in their life span whereas the more heterogeneous populations will show a continually developing fraction of $p16^{INK4a}$-positive senescent cells, some of which may be lost on passaging due to their reduced plating efficiency. A confounding factor, which is difficult to control for, is the change in cell size that takes place at senescence. This has the potential to mask increased expression of specific gene products when the analyses are conducted on equal amounts of total cellular protein [27]. Our impression is that the strains showing nonclassical $p16^{INK4a}$ accumulation generally have larger cells.

The open question is what determines whether a particular strain of fibroblast will show classical vs. nonclassical features. One obvious possibility we considered is the distinction between adult and fetal sources but this is untenable; the ESC cells derived from adult endometrium and the FDF cells derived from fetal skin both conformed to the classical pattern. Another possibility would be whether the cells were isolated from skin as opposed to other organs but again this does not hold as FDFs behaved differently from IDFs and other dermal strains. The most plausible correlation thus far is that the cells showing a nonclassical pattern of $p16^{INK4a}$ accumulation were all derived from external body sites, perhaps reflecting exposure to the environment, whereas the three examples of classical strains came from internal sites (including fetal skin), that would not have been exposed to environmental stress before tissue culture. Clearly, this hypothesis will require further evaluation by examining additional fibroblast strains isolated from internal body sites.

Fibroblasts at surface-exposed sites may be directly vulnerable to DNA damage or they may be called upon to proliferate stochastically in reaction to radiation, chemical or physical insults. If so, then pools of fibroblasts explanted from such sites might be expected to display greater heterogeneity in telomere length than cells from internal sites. However, it remains a matter of debate whether the telomere signal that triggers M1 reflects the average telomere length, the presence of a single or limited number of short telomeres or the frequency with which telomeres undergo capping and uncapping [10,32,59–62]. The telomere capping model has the appeal that it can more readily explain the stochastic nature of senescence observed at the level of the individual cell. Thus, division of a single cell can result in progeny with very different proliferative potentials [63,64]. It also has echoes in the apparently stochastic up-regulation of $p16^{INK4a}$ that we report here but the mechanistic relationship between telomere dysfunction and $p16^{INK4a}$ regulation clearly requires further research.

Acknowledgments

We are grateful to Nico Smit, Wilma Bergman, Nelleke Gruis, Jan Brosens, Veronique Bataille, Anthony Quinn, Marie-Françoise Avril, Laurent Ferradini, Brigitte Bressac and Jean-Laurent Casanova for provision of cell cultures. We also thank David Wynford-Thomas, Robert Brooks and Julie Cooper for helpful discussions and comments on the manuscript.

References

[1] L. Hayflick, P.S. Moorhead, The serial cultivation of human diploid cell strains, Exp. Cell Res. 25 (1961) 585–621.
[2] J.W. Shay, W.E. Wright, H. Werbin, Defining the molecular mechanisms of human cell immortalization, Biochim. Biophys. Acta 1072 (1991) 1–7.
[3] W. Wei, J.M. Sedivy, Differentiation between senescence (M1) and crisis (M2) in human fibroblast cultures, Exp. Cell Res. 253 (1999) 519–522.
[4] G.P. Dimri, X. Lee, G. Basile, M. Acosta, G. Scott, C. Roskelley, E.E. Medrano, M. Linskens, I. Rubelj, O. Pereira-Smith, M. Peacocke, J. Campisi, A novel biomarker identifies senescent human cells in culture and in aging skin in vivo, Proc. Natl. Acad. Sci. U. S. A. 92 (1995) 9363–9367.
[5] C.B. Harley, Telomere loss: mitotic clock or genetic time bomb? Mutat. Res. 256 (1991) 271–282.
[6] J.M. Sedivy, Can ends justify the means?: telomeres and the mechanisms of replicative senescence and immortalization in mammalian cells, Proc. Natl. Acad. Sci. U. S. A. 95 (1998) 9078–9081.
[7] W. Wright, J.W. Shay, Telomere dynamics in cancer progression and prevention: fundamental differences in human and mouse telomere biology, Nat. Med. 6 (2000) 849–851.
[8] A.G. Bodnar, M. Ouellette, M. Frolkis, S.E. Holt, C.-P. Chiu, G.B. Morin, C.B. Harley, J.W. Shay, S. Lichsteiner, W.E. Wright, Extension of life-span by introduction of telomerase into normal human cells, Science 279 (1998) 349–352.
[9] H. Vaziri, S. Benchimol, Reconstitution of telomerase activity in normal human cells leads to elongation of telomeres and extended replicative lifespan, Curr. Biol. 8 (1998) 279–282.
[10] W.E. Wright, J.W. Shay, Historical claims and current interpretations of replicative aging, Nat. Biotechnol. 20 (2002) 682–688.
[11] T. Kiyono, S.A. Foster, J.I. Koop, J.K. McDougall, D.A. Galloway, A.J. Klingelhutz, Both Rb/p16^{INK4a} inactivation and telomerase activity are required to immortalize human epithelial cells, Nature 396 (1998) 84–88.
[12] C.J. Jones, D. Kipling, M. Morris, P. Hepburn, J. Skinner, A. Bounacer, F.S. Wyllie, M. Ivan, J. Bartek, D. Wynford-Thomas, J.A. Bond, Evidence for a telomere-independent "clock" limiting *RAS* oncogene-driven proliferation of human thyroid epithelial cells, Mol. Cell. Biol. 20 (2000) 5690–5699.
[13] M.A. Dickson, W.C. Hahn, Y. Ino, V. Ronfard, J.Y. Wu, R.A. Weinberg, D.N. Louis, F.P. Li, J.G. Rheinwald, Human keratinocytes that express hTERT and also bypass a p16^{INK4a}-enforced mechanism that limits life span become immortal yet retain normal growth and differentiation characteristics, Mol. Cell. Biol. 20 (2000) 1436–1447.
[14] R.D. Ramirez, C.P. Morales, B.-S. Herbert, J.M. Rohde, C. Passons, J.W. Shay, W.E. Wright, Putative telomere-independent mechanisms of replicative aging reflect inadequate growth conditions, Genes Dev. 15 (2001) 398–403.
[15] D.F. Jarrard, S. Sarkar, Y. Shi, T.R. Yeager, G. Magrane, H. Kinoshita, N. Nassif, L. Meisner, M.A. Newton, F.M. Waldman, C.A. Reznikoff, p16/pRb pathway alterations are required for bypassing senescence in human prostate epithelial cells, Cancer Res. 59 (1999) 2957–2964.
[16] C. Sandhu, D.M. Peehl, J. Slingerland, p16^{INK4a} mediates cyclin dependent kinase 4 and 6 inhibition in senescent prostatic epithelial cells, Cancer Res. 60 (2000) 2616–2622.
[17] C.J. Sherr, R.A. DePinho, Cellular senescence: mitotic clock or culture shock? Cell 102 (2000) 407–410.
[18] Q. Chen, A. Fischer, J.D. Reagan, L.J. Yan, B.N. Ames, Oxidative DNA damage and senescence of human diploid fibroblast cells, Proc. Natl. Acad. Sci. U. S. A. 92 (1995) 4337–4341.
[19] R.H. te Poele, A.L. Okorokov, L. Jardine, J. Cummings, S.P. Joel, DNA damage is able to induce senescence in tumor cells in vitro and in vivo, Cancer Res. 62 (2002) 1876–1883.
[20] B.-D. Chang, E.V. Broude, M. Dokmanovic, H. Zhu, A. Ruth, Y. Xuan, E.S. Kandel, E. Lusch, K. Christov, I.B. Roninson, A senescence-like phenotype distinguishes tumor cells that undergo terminal proliferation arrest after exposure to anticancer agents, Cancer Res. 59 (1999) 3761–3767.
[21] C.A. Schmitt, J.S. Fridman, M. Yang, S. Lee, E. Baranov, R.M. Hoffman, S.W. Lowe, A senescence program controlled by p53 and p16^{INK4a} contributes to the outcome of cancer therapy, Cell 109 (2002) 335–346.
[22] M. Serrano, A.W. Lin, M.E. McCurrach, D. Beach, S.W. Lowe, Oncogenic *ras* provokes premature cell senescence associated with accumulation of p53 and p16^{INK4a}, Cell 88 (1997) 593–602.
[23] S. Drayton, J. Rowe, R. Jones, R. Vatcheva, D. Cuthbert-Heavens, J. Marshall, M. Fried, G. Peters, Tumor suppressor p16^{INK4a} determines sensitivity of human cells to transformation by cooperating cellular oncogenes, Cancer Cell 4 (2003) 301–310.
[24] S. Drayton, G. Peters, Immortalisation and transformation revisited, Curr. Opin. Genet. Dev. 12 (2002) 98–104.
[25] J.W. Shay, O.M. Pereira-Smith, W.E. Wright, A role for both RB and p53 in the regulation of human cellular senescence, Exp. Cell Res. 196 (1991) 33–39.
[26] E. Hara, H. Tsurui, A. Shinozaki, S. Nakada, K. Oda, Cooperative effect of antisense-Rb and antisense-p53 oligomers on the extension of life span of human diploid fibroblasts, TIG-1, Biochem. Biophys. Res. Commun. 179 (1991) 528–534.
[27] D.A. Alcorta, Y. Xiong, D. Phelps, G. Hannon, D. Beach, J.C. Barrett, Involvement of the cyclin-dependent kinase inhibitor p16 (INK4a) in replicative senescence, Proc. Natl. Acad. Sci. U. S. A. 93 (1996) 13742–13747.
[28] E. Hara, R. Smith, D. Parry, H. Tahara, S. Stone, G. Peters, Regulation of p16^{CDKN2} expression and its implications for cell immortalization and senescence, Mol. Cell. Biol. 16 (1996) 859–867.
[29] B.B. McConnell, M. Starborg, S. Brookes, G. Peters, Inhibitors of cyclin-dependent kinases induce features of replicative senescence in early passage human diploid fibroblasts, Curr. Biol. 8 (1998) 351–354.
[30] G.H. Stein, L.F. Drullinger, A. Soulard, V. Dulic, Differential roles for cyclin-dependent kinase inhibitors p21 and p16 in the mechanisms of senescence and differentiation in human fibroblasts, Mol. Cell. Biol. 19 (1999) 2109–2117.
[31] C.M. Counter, W.C. Hahn, W. Wei, S.D. Caddle, R.L. Beijersbergen, P.M. Lansdorp, J.M. Sedivy, R.A. Weinberg, Dissociation among in vitro telomerase activity, telomere maintenance, and cellular transformation, Proc. Natl. Acad. Sci. U. S. A. 95 (1998) 14723–14728.
[32] J. Zhu, H. Wang, J.M. Bishop, E.H. Blackburn, Telomerase extends the lifespan of virus-transformed human cells without net telomere lengthening, Proc. Natl. Acad. Sci. U. S. A. 96 (1999) 3723–3728.
[33] C.M. Beausejour, A. Krtolica, F. Galimi, M. Narita, S.W. Lowe, P. Yaswen, J. Campisi, Reversal of human cellular senescence: roles of the p53 and p16 pathways, EMBO J. 22 (2003) 4212–4222.
[34] M. Ruas, G. Peters, The p16^{INK4a}/CDKN2A tumor suppressor and its relatives, Biochim. Biophys. Acta 1378 (1998) 115–177.
[35] M. Morris, P. Hepburn, D. Wynford-Thomas, Sequential extension of proliferative lifespan in human fibroblasts induced by over-expres-

sion of CDK4 or 6 and loss of p53 function, Oncogene 21 (2002) 4277–4288.
[36] R.D. Ramirez, B.-S. Herbert, M.B. Vaughan, Y. Zou, K. Gandia, C.P. Morales, W.E. Wright, J.W. Shay, Bypass of telomere-dependent replicative senescence (M1) upon overexpression of Cdk4 in normal human epithelial cells, Oncogene 22 (2003) 433–444.
[37] J.J.L. Jacobs, K. Kieboom, S. Marino, R.A. DePinho, M. van Lohuizen, The oncogene and Polycomb-group gene *bmi-1* regulates cell proliferation and senescence through the *ink4a* locus, Nature 397 (1999) 164–168.
[38] K. Itahana, Y. Zou, Y. Itahana, J.-L. Martinez, C. Beausejour, J.J.L. Jacobs, M. van Lohuizen, V. Band, J. Campisi, G.P. Dimri, Control of the replicative life span of human fibroblasts by p16 and the polycomb protein Bmi-1, Mol. Cell. Biol. 23 (2003) 389–401.
[39] J. Duan, Z. Zhang, T. Tong, Senescence delay of human diploid fibroblasts induced by anti-sense $p16^{INK4a}$ expression, J. Biol. Chem. 276 (2001) 48325–48331.
[40] M. Narita, S. Nunez, E. Heard, M. Narita, A.W. Lin, S.A. Hearn, D.L. Spector, G.J. Hannon, S.W. Lowe, Rb-mediated heterochromatin formation and silencing of E2F target genes during cellular senescence, Cell 113 (2003) 703–716.
[41] M. Voorhoeve, R. Agami, The tumor-suppressive functions of the human *INK4A* locus, Cancer Cell 4 (2003) 311–319.
[42] W. Wei, U. Herbig, A. Dutriaux, J.M. Sedivy, Loss of retinoblastoma but not p16 function allows bypass of replicative senescence in human fibroblasts, EMBO Rep. 4 (2003) 1061–1066.
[43] J. Bond, C. Jones, M. Haughton, C. DeMicco, D. Kipling, D. Wynford-Thomas, Direct evidence from siRNA-directed "knock down" that $p16^{INK4a}$ is required for human fibroblast senescence and for limiting ras-induced epithelial cell proliferation, Exp. Cell Res. 292 (2004) 151–156.
[44] S. Brookes, J. Rowe, M. Ruas, S. Llanos, P.A. Clark, M. Lomax, M.C. James, R. Vatcheva, S. Bates, K.H. Vousden, D. Parry, N. Smit, N. Smit, W. Bergman, G. Peters, INK4a-deficient human diploid fibroblasts are resistant to RAS-induced senescence, EMBO J. 21 (2002) 2936–2945.
[45] T.J. Huot, J. Rowe, M. Harland, S. Drayton, S. Brookes, C. Goopta, P. Purkis, M. Fried, V. Bataille, E. Hara, J. Newton-Bishop, G. Peters, Biallelic mutations in $p16^{INK4a}$ confer resistance to Ras- and Ets-induced senescence in human diploid fibroblasts, Mol. Cell. Biol. 22 (2002) 8135–8143.
[46] F.J. Stott, S. Bates, M.C. James, B.B. McConnell, M. Starborg, S. Brookes, I. Palmero, E. Hara, K.H. Vousden, G. Peters, The alternative product from the human *CDKN2A* locus, $p14^{ARF}$, participates in a regulatory feedback loop with p53 and MDM2, EMBO J. 17 (1998) 5001–5014.
[47] N.A. Gruis, P.A. van der Velden, L.A. Sandkuiji, D.E. Prins, J. Weaver-Feldhaus, A. Kamb, W. Bergman, R.R. Frants, Homozygotes for *CDKN2* (p16) germline mutations in Dutch familial melanoma kindreds, Nat. Genet. 10 (1995) 351–353.
[48] V.J. Cristofalo, R.G. Allen, R.J. Pignolo, B.G. Martin, J.C. Beck, Relationship between donor age and the replicative lifespan of human cells in culture: a reevaluation, Proc. Natl. Acad. Sci. U. S. A. 95 (1998) 10614–10619.
[49] E.L. Schneider, Y. Mitsui, The relationship between age of donor and in vitro life span of human diploid fibroblasts, Proc. Natl. Acad. Sci. U. S. A. 73 (1976) 3584–3588.
[50] G.M. Martin, C.A. Sprague, C.J. Epstein, Replicative life-span of cultivated human cells. Effects of donor's age, tissue and genotype, Lab. Invest. 23 (1970) 86–92.
[51] S. Goldstein, E.J. Moerman, J.S. Soeldner, R.E. Gleason, D.M. Barnett, Chronologic and physiologic age affect replicative life-span of fibroblasts from diabetic, prediabetic, and normal donors, Science 199 (1978) 781–782.
[52] J.A. Bond, M.F. Haughton, J.M. Rowson, P.J. Smith, V. Gire, S. Wynford-Thomas, F.S. Wyllie, Control of replicative life span in human cells: barriers to clonal expansion intermediate between M1 senescence and M2 crisis, Mol. Cell. Biol. 19 (1999) 3103–3114.
[53] J.A. Bond, F.S. Wyllie, D. Wynford-Thomas, Escape from senescence in human diploid fibroblasts induced directly by mutant p53, Oncogene 9 (1994) 1885–1889.
[54] W. Wei, R.M. Hemmer, J.M. Sedivy, The role of $p14^{ARF}$ in replicative and induced senescence of human fibroblasts, Mol. Cell. Biol. 21 (2001) 6748–6757.
[55] J.P. Brown, W. Wei, J.M. Sedivy, Bypass of senescence after disruption of $p21^{CIP1/WAF1}$ gene in normal diploid human fibroblasts, Science 277 (1997) 831–834.
[56] J.R. Noble, E.M. Rogan, A.A. Neumann, K. Maclean, T.M. Bryan, R.R. Reddel, Association of extended in vitro proliferative potential with loss of $p16^{INK4}$ expression, Oncogene 13 (1996) 1259–1268.
[57] C.J. Sherr, J.M. Roberts, CDK inhibitors: positive and negative regulators of G1-phase progression, Genes Dev. 13 (1999) 1501–1512.
[58] J.A. Baur, Y. Zou, J.W. Shay, W.E. Wright, Telomere position effect in human cells, Science 292 (2001) 2075–2077.
[59] E.H. Blackburn, Telomere states and cell fates, Nature 408 (2000) 53–56.
[60] M.T. Henman, M.A. Strong, L.-Y. Hao, C.W. Greider, The shortest telomere, not average telomere length, is critical for cell viability and chromosome stability, Cell 107 (2001) 67–77.
[61] J. Karlseder, A. Smogorzewska, T. de Lange, Senescence induced by altered telomere state, not telomere loss, Science 295 (2002) 2446–2449.
[62] U.M. Martens, E.A. Chavez, S.S.S. Poon, C. Schmoor, P.M. Lansdorp, Accumulation of short telomeres in human fibroblasts prior to replicative senescence, Exp. Cell Res. 256 (2000) 291–299.
[63] J.R. Smith, R.G. Whitney, Intraclonal variation in proliferative potential of human diploid fibroblasts: stochastic mechanisms for cellular aging, Science 207 (1980) 82–84.
[64] J. Pontén, W.D. Stein, S. Shall, A quantitative analysis of the aging of human glial cells in culture, J. Cell. Physiol. 117 (1983) 342–352.